

---

# Fast-WAM: Do World Action Models Need Test-time Future Imagination?

---

Tianyuan Yuan<sup>1,2</sup>, Zibin Dong<sup>1,2</sup>, Yicheng Liu<sup>1,2</sup>, Hang Zhao<sup>1,2</sup>

<sup>1</sup>IIS, Tsinghua University    <sup>2</sup>Galaxea AI

<https://yuantianyuan01.github.io/FastWAM/>

## Abstract

World Action Models (WAMs) have emerged as a promising alternative to Vision-Language-Action (VLA) models for embodied control because they explicitly model how visual observations may evolve under action. Most existing WAMs follow an imagine-then-execute paradigm, incurring substantial test-time latency from iterative video denoising, yet it remains unclear whether explicit future imagination is actually necessary for strong action performance.

In this paper, we ask whether WAMs need explicit future imagination at test time, or whether their benefit comes primarily from video modeling during training. We disentangle the role of video modeling during training from explicit future generation during inference by proposing **Fast-WAM**, a WAM architecture that retains video co-training during training but skips future prediction at test time. We further instantiate several Fast-WAM variants to enable a controlled comparison of these two factors. Across these variants, we find that Fast-WAM remains competitive with imagine-then-execute variants, while removing video co-training causes a much larger performance drop. Empirically, Fast-WAM achieves competitive results with state-of-the-art methods both on simulation benchmarks (LIBERO and RoboTwin) and real-world tasks, without embodied pretraining. It runs in real time with 190 ms latency, over  $4\times$  faster than existing imagine-then-execute WAMs. These results suggest that the main value of video prediction in WAMs may lie in improving world representations during training rather than generating future observations at test time.

## 1 Introduction

Building general-purpose embodied agents requires policies that can not only map visual observations to actions, but also reason about how the physical world evolves under interaction. This has motivated growing interest in World Action Models (WAMs), which combine future visual prediction and action modeling in a unified framework. Compared with standard Vision-Language-Action (VLA) models, WAMs are appealing because modeling future observations may help capture physical dynamics and task-relevant temporal structure.

Most existing WAMs follow an imagine-then-execute paradigm: they first generate future observations, then predict actions conditioned on the imagined future. While intuitive, this design incurs substantial test-time latency due to iterative video denoising [1, 2, 3, 4, 5]. More fundamentally, it remains unclear whether explicit future imagination is actually necessary for strong action performance. The effectiveness of WAMs may stem from two distinct sources: (1) the video prediction objective during training, which may help the model acquire stronger physical priors and action-conditioned representations, and (2) explicit future generation during inference, which may provide additional foresight for action prediction. Existing WAM systems typically entangle these two factors, making it difficult to determine which one is actually responsible for the observed gains.

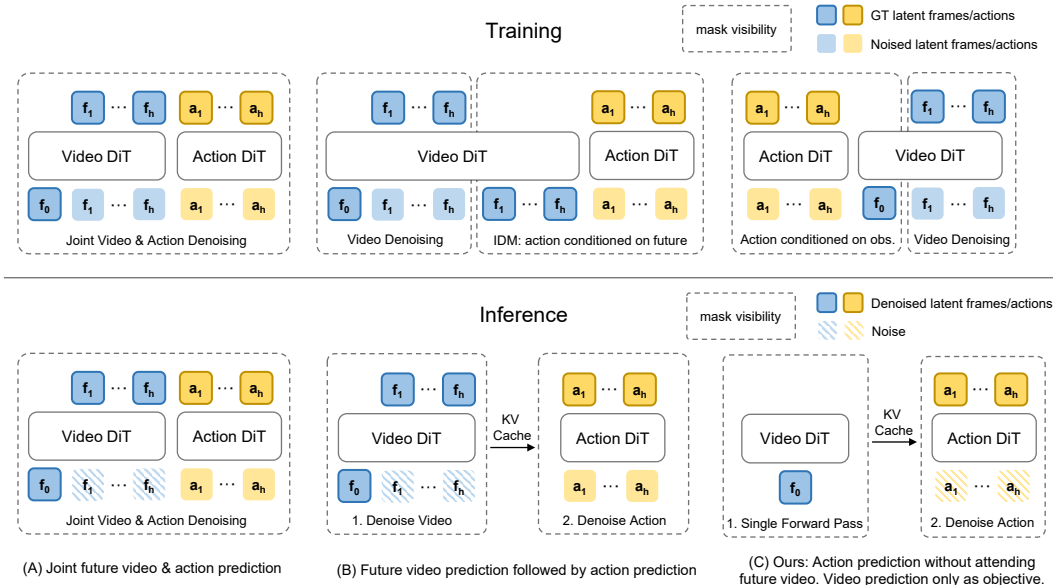


Figure 1: Three representative WAM paradigms. (A) Joint-modeling WAMs denoise future video and action tokens together. (B) Causal WAMs first generate future observations and then condition action prediction on the generated future representation. (C) Fast-WAM retains video co-training during training but removes explicit future generation at inference time, directly predicting actions from latent world representations in a single forward pass.

In this paper, we revisit this design choice and ask a simple question: *do WAMs need to imagine future observations at test time, or do they benefit primarily from learning to model them during training?* Our key idea is to decouple the video prediction objective used in WAM training from explicit future generation at inference time. If the main value of world modeling lies in shaping better latent representations during training, then a WAM should be able to retain this benefit without paying the test-time cost of future video synthesis.

Based on this perspective, we propose **Fast-WAM**, a WAM architecture that preserves video co-training during training but skips future prediction at test time. Instead of using a pretrained video generation model to iteratively synthesize future frames during inference, Fast-WAM repurposes a pretrained video Diffusion Transformer (DiT) as a single-pass world encoder for action generation. Concretely, we build Fast-WAM with a Mixture-of-Transformer (MoT) architecture with shared attention, consisting of a video DiT and an action expert DiT, as illustrated in Figure 1(C). During training, the video prediction objective shapes the video DiT to encode physically meaningful motion and interaction structure. During inference, the video DiT processes the observation context in a single forward pass and provides latent world representations for action denoising, avoiding explicit future video denoising and enabling efficient real-time control.

To study our central question in a controlled way, we instantiate Fast-WAM into variants that mirror representative imagine-then-execute WAM designs. For simplicity, we focus on single action chunk generation and omit the outer auto-regressive loop. As shown in Figure 1, existing WAMs can be broadly grouped into two representative paradigms: (A) future videos and actions are jointly denoised with shared attention [4, 6, 5]; and (B) actions are predicted after, and conditioned on, generated future videos [3, 7, 8]. We also implement a no-video-co-training variant, which serves as a direct control for the role of the training objective itself. Together, these controlled comparisons allow us to isolate the contribution of test-time future imagination from that of video co-training during training.

Experiments on simulation benchmarks (LIBERO and RoboTwin) show that Fast-WAM achieves strong results without any embodied pretraining, demonstrating strong data efficiency. On real-world robotic tasks, Fast-WAM remains highly effective while running at only 190 ms latency, making it more than  $4\times$  faster than existing imagine-then-execute WAM approaches. More importantly, controlled comparisons show that Fast-WAM stays close to imagine-then-execute variants, while removing the video co-training objective causes a much larger performance drop. These results

suggest that the main value of video prediction in WAMs may lie in improving world representations during training rather than in explicitly generating future observations at test time.

Our contributions are three-fold:

- We identify and study a basic question in WAMs: whether their gains come primarily from video modeling during training or from explicit future imagination during inference.
- We propose Fast-WAM, a WAM architecture that retains video co-training during training while eliminating future prediction at test time, enabling real-time inference.
- Through controlled comparisons on simulation and real-world benchmarks, including variants with and without video co-training, we show that much of the benefit of WAMs comes from the video co-training objective itself, while explicit future generation at inference time appears to be less critical than previously assumed.

## 2 Related Work

**Vision-Language-Action Policies.** Recent progress in embodied foundation models has been driven by Vision-Language-Action (VLA) policies, which directly map visual observations and language instructions to robot actions using large pretrained vision-language backbones [9, 10, 11, 12, 13, 14, 15, 16, 17, 18, 19]. By inheriting strong semantic priors from web-scale pretraining, these models have shown strong generalization across objects, scenes, and language instructions. However, as noted in recent WAM work, standard VLA pretraining is largely based on static image-text data and does not explicitly model how the physical world evolves under action [3, 4]. Our work is complementary to this line: Fast-WAM preserves a direct-policy interface at test time, similar to VLAs, but learns it under an additional world-modeling objective based on future visual prediction.

**World Action Models and Video-based Robot Policies.** A parallel line of work studies robot control through future visual prediction, using video generation as a way to model environment dynamics and infer actions [8, 20, 21, 7, 22, 23, 24, 25, 26, 27, 28, 29, 30, 31]. Recent methods further scale this idea by jointly modeling future video and robot actions in a unified framework [6, 2, 32, 33, 1, 3, 5, 4]. We follow [4] to refer to these models as World Action Models (WAMs), since they leverage world modeling, i.e., predicting future visual states, to support downstream action prediction. Most existing WAMs either follow an imagine-then-execute paradigm, where future visual trajectories are first generated and then used for action prediction, or jointly model future video and actions within a shared generative process. Our work is most closely related to this line, but differs in focus: rather than proposing another imagine-then-execute WAM, we study whether the gains of WAMs come primarily from video co-training during training or from explicit future imagination during inference.

Our work is also related to recent efforts that exploit video modeling for action prediction while reducing or bypassing explicit test-time video synthesis. VPP [34] conditions robot policies on predictive visual representations extracted from a video diffusion model, while UVA [35] jointly models video and action and skips video decoding at test time for faster inference. Compared with these works, our focus is on disentangling the relative roles of training-time video co-training and test-time future imagination through controlled variants under a shared framework.

## 3 Method

### 3.1 Problem Formulation

We consider embodied policy learning from visual observations and language instructions. Let  $o$  denote the current observation,  $l$  denote the task instruction, and  $a_{1:H}$  denote an action chunk of horizon  $H$ . A standard visuomotor policy models the conditional distribution

$$p(a_{1:H} \mid o, l), \tag{1}$$

which directly maps the current perceptual context to a sequence of actions. World Action Models (WAMs) augment this formulation by introducing future visual observations as an intermediate

variable. Let  $v_{1:T}$  denote future visual observations over a prediction horizon  $T$ . Many existing WAMs follow an *imagine-then-execute* factorization:

$$p(a_{1:H} | o, l) = \int p(v_{1:T} | o, l) p(a_{1:H} | o, l, v_{1:T}) dv_{1:T}, \quad (2)$$

where the model first predicts future observations and then conditions action generation on the imagined future. In practice, this is typically implemented either by jointly denoising future video and actions within a shared model, or by first generating future video and then feeding it to an inverse dynamics or action prediction module. Some prior WAMs further wrap this formulation in an outer auto-regressive rollout, which we omit here for simplicity and controlled comparison.

Our starting point is the observation that the effectiveness of WAMs may arise from two distinct factors: (i) the video prediction objective used during training, which can encourage the model to learn physically meaningful latent representations, and (ii) explicit future generation during inference, which may provide additional foresight for action prediction. Existing WAM formulations usually couple these two factors, since the same model both learns from future video prediction and explicitly synthesizes future observations at test time. We design Fast-WAM to decouple these two factors. During training, it retains world modeling as a co-training signal; during inference, however, it does not explicitly generate future observations. Instead, Fast-WAM predicts actions directly from the current observation and instruction,

$$p_{\theta}(a_{1:H} | o, l), \quad (3)$$

while using latent world representations shaped by video co-training. In this sense, Fast-WAM has a direct-policy interface at test time, similar to standard VLA policies, while its representation learning remains grounded in WAM-style video modeling during training. Formally, let  $z(o, l)$  denote the latent world representation produced by the video backbone conditioned on the current context. Fast-WAM uses this representation to parameterize the action distribution,

$$p_{\theta}(a_{1:H} | o, l) = p_{\theta}(a_{1:H} | z(o, l)). \quad (4)$$

The key difference from imagine-then-execute WAMs is that  $z(o, l)$  is obtained by a single forward encoding pass, rather than by explicitly sampling or denoising future observations  $v_{1:T}$  at inference time.

### 3.2 Model Architecture

**Overview.** Fast-WAM is designed to preserve the training benefits of world modeling while removing the inference cost of explicit future imagination. During training, it jointly learns action prediction and video modeling, encouraging the visual backbone to capture physically meaningful motion and interaction structure. During inference, Fast-WAM does not explicitly generate future observations. Instead, it keeps only the clean latent tokens of the first observation frame, processes them with the video model in a single forward pass, and uses the resulting latent world representation for direct action generation. This gives Fast-WAM a direct-policy interface at test time while retaining WAM-style video supervision during training.

**Architecture.** Fast-WAM is built on top of the video Diffusion Transformer (DiT) from Wan2.2-5B [36], which serves as the world modeling backbone. We also reuse its pretrained text encoder and video VAE: task language is encoded by the built-in T5 encoder and provided to all tokens through cross-attention, while visual observations are mapped into latent video tokens by the pretrained VAE. On top of this backbone, we introduce an action expert DiT for action chunk generation. The full model is organized as a Mixture-of-Transformer (MoT) architecture with shared attention between the video and action branches, as illustrated in Figure 2a.

We organize the input tokens into three groups: clean latent tokens of the first observation frame, which serve as the shared visual anchor; noisy latent tokens of future video frames, which are used only during training for video modeling; and action tokens, which are processed by the action expert for action generation. All token groups attend to the language embeddings through cross-attention. A structured attention mask controls the information flow between these groups. During training, future noisy video tokens attend bidirectionally within the video branch and can access the clean first-frame tokens; action tokens attend bidirectionally within the action branch and can also access the clean first-frame tokens. Crucially, action tokens cannot attend to future video tokens, and the

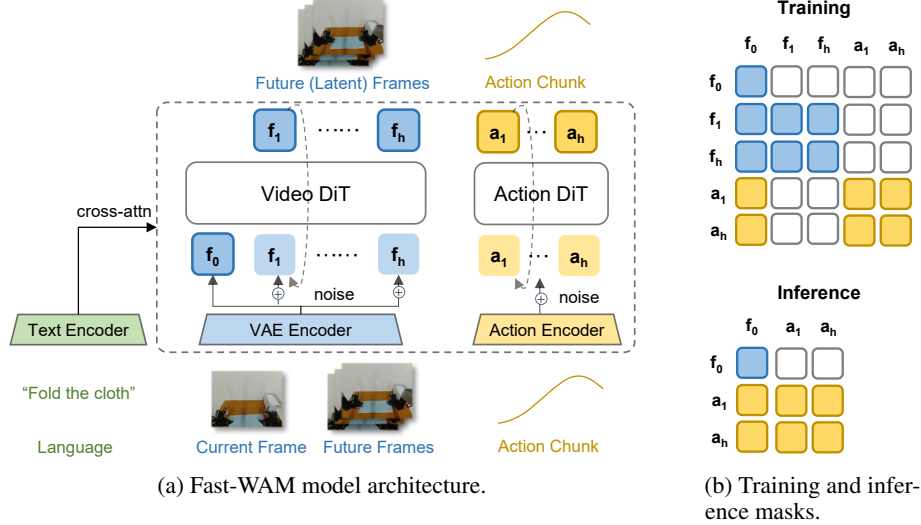


Figure 2: Fast-WAM architecture and the structured attention mask used to disentangle video co-training from action generation.

clean first-frame tokens do not attend to any other tokens. This ensures that both video modeling and action prediction are grounded in the same visual context while preventing future information from leaking into the action branch. We provide the full training and inference masks in Figure 2b.

At inference time, Fast-WAM removes the future video branch entirely: only the clean first-frame latent tokens are retained and passed through the video backbone once to produce latent world features for the action expert. Since no future noisy video tokens are instantiated and no explicit future video denoising is performed, Fast-WAM incurs substantially lower inference cost than standard imagine-then-execute WAMs.

**Training objective.** Fast-WAM is trained with a joint flow matching objective over action tokens and future video latents. Given a target variable  $y$  (either an action chunk  $a_{1:H}$  or future video latents  $z_{1:T}$ ), we sample Gaussian noise  $\epsilon \sim \mathcal{N}(0, I)$  and a time step  $t \in (0, 1)$ , and construct the interpolated sample

$$y_t = (1 - t)y + t\epsilon. \quad (5)$$

The model is trained to predict the corresponding velocity field with a standard flow matching objective

$$\mathcal{L}_{\text{FM}}(y) = \mathbb{E}_{y, \epsilon, t} \left[ \|f_{\theta}(y_t, t, o, l) - (\epsilon - y)\|_2^2 \right]. \quad (6)$$

We instantiate this objective for both action generation and video co-training. For action prediction, we set  $y = a_{1:H}$  and optimize

$$\mathcal{L}_{\text{act}} = \mathcal{L}_{\text{FM}}(a_{1:H}). \quad (7)$$

For video co-training, we set  $y = z_{1:T}$ , where  $z_{1:T}$  denotes the latent tokens of future video frames produced by the pretrained VAE, and optimize

$$\mathcal{L}_{\text{vid}} = \mathcal{L}_{\text{FM}}(z_{1:T}). \quad (8)$$

The overall training objective is

$$\mathcal{L} = \mathcal{L}_{\text{act}} + \lambda \mathcal{L}_{\text{vid}}, \quad (9)$$

where  $\lambda$  balances action learning and video co-training.

### 3.3 Controlled Variants for Disentangled WAM Design

To answer our central question, namely whether the benefit of WAMs comes primarily from video co-training during training or from explicit future imagination during inference, we design a set of controlled variants under a shared implementation framework. We instantiate representative

imagine-then-execute design patterns from recent WAMs while keeping the backbone, tokenization, and training recipe as aligned as possible. This controlled setup allows us to isolate the contribution of test-time future generation from that of the video co-training objective itself.

As illustrated in Figure 1(A) and (B), we consider two representative imagine-then-execute variants that capture the dominant design patterns in recent WAMs. The first variant, named Fast-WAM-Joint, follows the joint-generation paradigm, where future video tokens and action tokens are denoised together within a shared model, so that action generation remains coupled with future video modeling throughout the denoising process [4, 6, 5]. The second variant, named Fast-WAM-IDM, follows the video-then-action paradigm, where future video tokens are generated first from the current observation and language context, and action prediction is then conditioned on the resulting future representation [3, 7, 8]. In both cases, we preserve the defining inference structure of the corresponding paradigm, together with key training choices used in recent WAMs, while implementing them within our shared framework for controlled comparison with Fast-WAM.

We further construct a Fast-WAM variant without video co-training. This variant keeps the architecture and inference procedure unchanged, and removes only the video modeling objective during training. It therefore serves as a direct control for the role of video co-training itself. Together, these controlled variants isolate the two factors that are typically entangled in prior WAMs: video co-training during training and explicit future imagination during inference.

## 4 Experiment

### 4.1 Implementation Details

We use pretrained Wan2.2-5B [36] as the backbone, including its video DiT, text encoder, and video VAE. The action expert shares the same architecture as the video branch but uses a reduced hidden dimension of  $d_a = 1024$ , resulting in a 1B action expert and a total model size of 6B parameters. We set the action horizon to  $h = 32$ . Video frames are temporally downsampled by  $4\times$ , resulting in 9 video frames per chunk. Images from multiple cameras are concatenated into a single image before being fed into the VAE.

We use the same flow-matching formulation for both the video and action branches. Following [36], we adopt a logit-normal distribution over  $t$  as the noise schedule during both training and inference. During inference, we use 10 denoising steps with classifier-free guidance (CFG) scale set to 1.0. We use AdamW with a learning rate of  $1 \times 10^{-4}$ , weight decay of 0.01, and a cosine annealing schedule for all training settings. Training is conducted in mixed precision with gradient clipping at 1.0. All latency numbers are measured on a single NVIDIA RTX 5090D V2 32GB GPU.

We build Fast-WAM-Joint by allowing attention between video and action tokens. For Fast-WAM-IDM, we follow [3] and apply noise augmentation to the ground-truth video tokens with probability  $p = 0.5$ .

### 4.2 Experiment Setup

We evaluate Fast-WAM and its variants on both simulation benchmarks, namely LIBERO [37] and RoboTwin 2.0 [38], as well as on a real-world manipulation task.

**LIBERO.** We follow the standard benchmarking protocol and train our models on the four LIBERO suites: LIBERO-Spatial, LIBERO-Object, LIBERO-Goal, and LIBERO-Long. Each suite contains 500 demonstrations spanning 10 tasks. All models are trained for 20k steps. We report success rates for each suite, evaluated over a total of 2000 trials across 40 tasks with different random seeds.

**RoboTwin 2.0.** RoboTwin 2.0 is a challenging bimanual manipulation benchmark featuring more than 50 tasks that require coordinated dual-arm control. We follow the multi-task training setup of [5, 3], where models are trained on a mixture of 2,500 demonstrations collected in clean scenes and 25,000 demonstrations collected under heavy scene randomization, spanning over 50 tasks. All models are trained for 30k steps. We report average success rates over 100 trials per task under both clean and randomized settings.

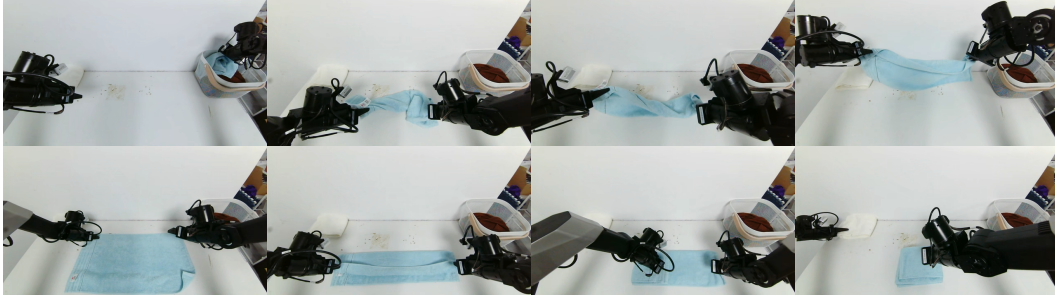


Figure 3: Real-world towel-folding task on the Galaxea R1 Lite platform. Folding a deformable object requires long-horizon planning and precise closed-loop manipulation, making it a challenging benchmark for evaluating both task success and execution efficiency.

Table 1: Results on RoboTwin. Fast-WAM matches strong pretrained WAM baselines without using embodied pretraining, while the two imagine-then-execute variants remain highly comparable and removing video co-training causes a substantial drop.

Method	Embodied PT.	Clean	Rand.	Average
$\pi_0$ [10]	✓	65.92	58.40	62.2
$\pi_{0.5}$ [11]	✓	82.74	76.76	79.8
Motus [5]	✓	88.66	87.02	87.8
Motus from WAN2.2	✗	77.56	77.00	77.3
LingBot-VA [3]	✓	92.90	91.50	<b>92.2</b>
LingBot-VA from WAN2.2	✗	80.60	–	80.6
<b>Fast-WAM (Ours)</b>	✗	91.88	91.78	<u>91.8</u>
<i>Fast-WAM Variants</i>				
Fast-WAM	✗	91.88	91.78	<b>91.8</b>
Fast-WAM-Joint	✗	90.84	90.32	90.6
Fast-WAM-IDM	✗	91.16	91.34	<u>91.3</u>
Fast-WAM w.o. video co-train	✗	82.76	84.80	83.8

**Real-World Evaluation.** We conduct real-world evaluation on towel folding, a long-horizon and challenging task that requires the policy to reason about the dynamics of deformable objects, as shown in Figure 3. We collect 60 hours of teleoperated demonstrations on the Galaxea R1 Lite platform. All models are trained for 30k steps. We report both the average success rate and the average completion time. The former measures whether the policy can eventually complete the folding task given sufficient time, while the latter reflects whether the policy learns an efficient execution strategy rather than relying on repeated trial-and-error corrections. For this task, completion time is therefore as important as success rate in assessing policy quality.

### 4.3 Main Results

#### 4.3.1 Overall comparison on simulation benchmarks

Table 1 and Table 2 summarize the results on RoboTwin and LIBERO, respectively. Overall, Fast-WAM achieves performance comparable to state-of-the-art methods on both benchmarks without using embodied pretraining. Per-task results on RoboTwin are listed in Appendix Table 3.

On RoboTwin, Fast-WAM achieves 91.8% success rate, exceeding all baselines without embodied pretraining and remaining highly competitive with the strongest pretrained WAMs. In particular, Fast-WAM substantially outperforms Motus [5] both with pretraining (87.8%) and without pretraining (77.3%), as well as LingBot-VA [3] without pretraining (80.6%), while remaining comparable to pretrained LingBot-VA (92.2%). These results suggest that Fast-WAM can recover most of the benefit of prior WAM pipelines without relying on embodied pretraining.

Table 2: Results on LIBERO. Fast-WAM achieves competitive overall performance without embodied pretraining, remains close to both imagine-then-execute variants, and outperforms the no-video-co-training ablation by a clear margin.

Method	Embodied PT.	Spatial	Object	Goal	Long	Average
OpenVLA [9]	✓	84.7	88.4	79.2	53.7	76.5
$\pi_0$ [10]	✓	96.8	98.8	95.8	85.2	94.1
$\pi_{0.5}$ [11]	✓	98.8	98.2	98.0	92.4	96.9
LingBot-VA [3]	✓	98.5	99.6	97.2	98.5	<b>98.5</b>
Motus [5]	✓	96.8	99.8	96.6	97.6	97.7
<b>Fast-WAM (Ours)</b>	✗	98.2	100.0	97.0	95.2	97.6
<i>Fast-WAM Variants</i>						
Fast-WAM	✗	98.2	100.0	97.0	95.2	97.6
Fast-WAM-Joint	✗	99.6	99.4	98.2	96.8	<b>98.5</b>
Fast-WAM-IDM	✗	98.8	97.8	97.8	97.6	<u>98.0</u>
Fast-WAM w.o. video co-train	✗	89.2	99.2	95.4	90.0	93.5

On LIBERO, Fast-WAM also delivers strong overall performance, achieving an average success rate of 97.6% without embodied pretraining. It outperforms the strong VLA baseline  $\pi_{0.5}$  and remains competitive with pretrained WAM baselines such as LingBot-VA (98.5%) and Motus (97.7%). These results show that Fast-WAM is consistently effective across diverse simulation benchmarks, even without the embodied pretraining used by most prior WAM and VLA baselines.

#### 4.3.2 Controlled comparison with Fast-WAM variants

We next compare Fast-WAM with the controlled variants introduced in Sec. 3.3 to disentangle the role of explicit future imagination at inference time from that of video co-training during training. Across both simulation benchmarks, the overall pattern is consistent: Fast-WAM remains comparable to the two imagine-then-execute variants, while removing video co-training leads to a much larger performance drop.

On RoboTwin, Fast-WAM achieves 91.8% success rate, which is highly comparable to both Fast-WAM-Joint (90.6%) and Fast-WAM-IDM (91.3%). In contrast, removing video co-training reduces performance to 83.8%, yielding a substantial gap relative to all three variants with video co-training. This result suggests that, on this benchmark, retaining the video modeling objective during training is far more important than explicitly generating future observations at test time. A similar trend holds on LIBERO. Fast-WAM reaches 97.6% average success rate, remaining close to Fast-WAM-Joint (98.5%) and Fast-WAM-IDM (98.0%). By comparison, Fast-WAM without video co-training drops to 93.5%, with especially visible degradation on the *Spatial* and *Long* subsets. Again, the gap caused by removing video co-training is clearly larger than the gap between Fast-WAM and the imagine-then-execute variants.

This pattern suggests that the main benefit of WAM-style training may lie less in whether, or how, future imagination is performed at test time, and more in the video prediction objective used to shape world-grounded representations during training.

#### 4.3.3 Real-world performance and efficiency

We further evaluate Fast-WAM on a long-horizon real-world towel-folding task. We report both the average success rate and the average completion time, as they capture two equally important aspects of policy quality: whether the policy can eventually complete the task, and whether it does so efficiently rather than through repeated trial-and-error corrections. Results are shown in Figure 4.

On this task, pretrained  $\pi_{0.5}$  remains the strongest method, achieving the highest success rate together with the shortest completion time. Among the Fast-WAM family, the overall performance is comparable, with Fast-WAM-IDM achieving the highest success rate, while Fast-WAM attains a better completion time. Importantly, all Fast-WAM variants with video co-training substantially outperform  $\pi_{0.5}$  without pretraining, indicating that WAM-style video co-training provides strong data efficiency even without embodied pretraining.

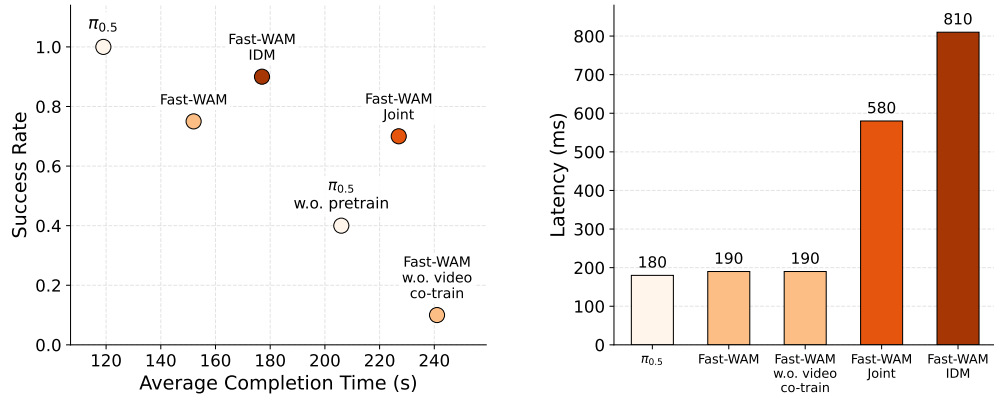


Figure 4: Real-world results on the long-horizon towel-folding task. The left panel plots success rate against average completion time, where upper-left is better. The right panel compares inference latency. Fast-WAM achieves strong real-world performance with substantially lower latency than imagine-then-execute variants, while removing video co-training degrades both success rate and completion time.

In contrast, removing video co-training causes a dramatic degradation on both metrics: Fast-WAM without video co-training drops to only 10% success rate and also requires the longest completion time among all methods. This gap is much larger than the differences among the Fast-WAM variants themselves, suggesting that video co-training is the dominant factor behind strong real-world performance, whereas the effect of test-time future imagination is comparatively limited.

In terms of runtime, Fast-WAM retains low inference latency (190 ms), whereas the imagine-then-execute variants are substantially slower, especially Fast-WAM-IDM at 810 ms. This makes Fast-WAM a more favorable design point for real-world deployment, offering strong task performance together with much lower inference cost.

## 5 Conclusion

In this paper, we revisited a basic question in World Action Models: whether their gains come primarily from explicit future imagination at test time or from video modeling during training. To study this question, we introduced Fast-WAM, a WAM architecture that retains video co-training during training while skipping future prediction at inference time, enabling direct action generation from world-grounded latent representations. Across simulation benchmarks and real-world robotic tasks, Fast-WAM achieves strong performance without embodied pretraining while running in real time. More importantly, controlled comparisons show that Fast-WAM remains competitive with imagine-then-execute variants, whereas removing video co-training leads to a much larger degradation. These results suggest that the main value of video prediction in WAMs may lie more in learning better world representations during training than in generating future observations at test time. An important direction for future work is to study the effect of larger-scale pretraining data and model scaling on this design.

## References

- [1] Jonas Pai, Liam Achenbach, Victoriano Montesinos, Benedek Forrai, Oier Mees, and Elvis Nava. *mimic-video: Video-action models for generalizable robot control beyond vlas*. *arXiv preprint 2512.15692*, 2025.
- [2] Junbang Liang, Pavel Tokmakov, Ruoshi Liu, Sruthi Sudhakar, Paarth Shah, Rares Ambrus, and Carl Vondrick. *Video generators are robot policies*. *arXiv preprint arXiv:2508.00795*, 2025.
- [3] Lin Li, Qihang Zhang, Yiming Luo, Shuai Yang, Ruilin Wang, Fei Han, Mingrui Yu, Zelin Gao, Nan Xue, Xing Zhu, Yujun Shen, and Yinghao Xu. *Causal world modeling for robot control*. *arXiv preprint arXiv:2601.21998*, 2026.
- [4] Seonghyeon Ye, Yunhao Ge, Kaiyuan Zheng, Shenyuan Gao, Sihyun Yu, George Kurian, Suneel Indupuru, You Liang Tan, Chuning Zhu, Jiannan Xiang, Ayaan Malik, Kyungmin Lee, William Liang, Nadun Ranawaka, Jiasheng Gu, Yinze Xu, Guanzhi Wang, Fengyuan Hu, Avnish Narayan, Johan Bjorck, Jing Wang, Gwanghyun Kim, Dantong Niu, Ruijie Zheng, Yuqi Xie, Jimmy Wu, Qi Wang, Ryan Julian, Danfei Xu, Yilun Du, Yevgen Chebotar, Scott Reed, Jan Kautz, Yuke Zhu, Linxi "Jim" Fan, and Joel Jang. *World action models are zero-shot policies*, 2026. URL <https://arxiv.org/abs/2602.15922>.
- [5] Hongzhe Bi, Hengkai Tan, Shenghao Xie, Zeyuan Wang, Shuhe Huang, Haitian Liu, Ruowen Zhao, Yao Feng, Chendong Xiang, Yinze Rong, Hongyan Zhao, Hanyu Liu, Zhizhong Su, Lei Ma, Hang Su, and Jun Zhu. *Motus: A unified latent action world model*, 2025. URL <https://arxiv.org/abs/2512.13030>.
- [6] Chuning Zhu, Raymond Yu, Siyuan Feng, Benjamin Burchfiel, Paarth Shah, and Abhishek Gupta. *Unified world models: Coupling video and action diffusion for pretraining on large robotic datasets*, 2025. URL <https://arxiv.org/abs/2504.02792>.
- [7] Yao Feng, Hengkai Tan, Xinyi Mao, Chendong Xiang, Guodong Liu, Shuhe Huang, Hang Su, and Jun Zhu. *Vidar: Embodied video diffusion model for generalist manipulation*, 2025. URL <https://arxiv.org/abs/2507.12898>.
- [8] Yilun Du, Mengjiao Yang, Bo Dai, Hanjun Dai, Ofir Nachum, Joshua B. Tenenbaum, Dale Schuurmans, and Pieter Abbeel. *Learning universal policies via text-guided video generation*, 2023. URL <https://arxiv.org/abs/2302.00111>.
- [9] Moo Jin Kim, Karl Pertsch, Siddharth Karamcheti, Ted Xiao, Ashwin Balakrishna, Suraj Nair, Rafael Rafailov, Ethan Foster, Grace Lam, Pannag Sanketi, et al. *Openvla: An open-source vision-language-action model*. *arXiv preprint arXiv:2406.09246*, 2024.
- [10] Kevin Black, Noah Brown, Danny Driess, Adnan Esmail, Michael Equi, Chelsea Finn, Niccolo Fusai, Lachy Groom, Karol Hausman, Brian Ichter, et al.  $\pi_0$ : A vision-language-action flow model for general robot control. *arXiv preprint arXiv:2410.24164*, 2024.
- [11] Physical Intelligence, Kevin Black, Noah Brown, James Darpinian, Karan Dhabalia, Danny Driess, Adnan Esmail, Michael Equi, Chelsea Finn, Niccolo Fusai, et al.  $\pi_{0.5}$ : a vision-language-action model with open-world generalization. *arXiv preprint arXiv:2504.16054*, 2025.
- [12] Johan Bjorck, Fernando Castañeda, Nikita Cherniadev, Xingye Da, Runyu Ding, Linxi Fan, Yu Fang, Dieter Fox, Fengyuan Hu, Spencer Huang, et al. *Gr00t n1: An open foundation model for generalist humanoid robots*. *arXiv preprint arXiv:2503.14734*, 2025.
- [13] Brianna Zitkovich, Tianhe Yu, Sichun Xu, Peng Xu, Ted Xiao, Fei Xia, Jialin Wu, Paul Wohlhart, Stefan Welker, Ayzaan Wahid, et al. *Rt-2: Vision-language-action models transfer web knowledge to robotic control*. In *Conference on Robot Learning*, pages 2165–2183. PMLR, 2023.
- [14] Songming Liu, Lingxuan Wu, Bangguo Li, Hengkai Tan, Huayu Chen, Zhengyi Wang, Ke Xu, Hang Su, and Jun Zhu. *Rdt-1b: a diffusion foundation model for bimanual manipulation*. *arXiv preprint arXiv:2410.07864*, 2024.

- [15] Qingwen Bu, Jisong Cai, Li Chen, Xiuqi Cui, Yan Ding, Siyuan Feng, Shenyuan Gao, Xindong He, Xuan Hu, Xu Huang, et al. Agibot world colosseum: A large-scale manipulation platform for scalable and intelligent embodied systems. *arXiv preprint arXiv:2503.06669*, 2025.
- [16] Mustafa Shukor, Dana Aubakirova, Francesco Capuano, Pepijn Kooijmans, Steven Palma, Adil Zouitine, Michel Aractingi, Caroline Pascal, Martino Russi, Andres Marafioti, et al. Smolvla: A vision-language-action model for affordable and efficient robotics. *arXiv preprint arXiv:2506.01844*, 2025.
- [17] Gemini Robotics Team, Saminda Abeyruwan, Joshua Ainslie, Jean-Baptiste Alayrac, Montserrat Gonzalez Arenas, Travis Armstrong, Ashwin Balakrishna, Robert Baruch, Maria Bauza, Michiel Blokzijl, et al. Gemini robotics: Bringing ai into the physical world. *arXiv preprint arXiv:2503.20020*, 2025.
- [18] Galaxea Team. Galaxea g0: Open-world dataset and dual-system vla model. *arXiv preprint arXiv:2509.00576v1*, 2025.
- [19] Junjie Wen, Yichen Zhu, Jinming Li, Zhibin Tang, Chaomin Shen, and Feifei Feng. Dexvla: Vision-language model with plug-in diffusion expert for general robot control. *arXiv preprint arXiv:2502.05855*, 2025.
- [20] Hongtao Wu, Ya Jing, Chilam Cheang, Guangzeng Chen, Jiafeng Xu, Xinghang Li, Minghuan Liu, Hang Li, and Tao Kong. Unleashing large-scale video generative pre-training for visual robot manipulation, 2023.
- [21] Siyuan Zhou, Yilun Du, Jiaben Chen, Yandong Li, Dit-Yan Yeung, and Chuang Gan. Robodreamer: Learning compositional world models for robot imagination. *arXiv preprint arXiv:2404.12377*, 2024.
- [22] Homanga Bharadhwaj, Debidatta Dwivedi, Abhinav Gupta, Shubham Tulsiani, Carl Doersch, Ted Xiao, Dhruv Shah, Fei Xia, Dorsa Sadigh, and Sean Kirmani. Gen2act: Human video generation in novel scenarios enables generalizable robot manipulation. *arXiv preprint arXiv:2409.16283*, 2024.
- [23] John Won, Kyungmin Lee, Huiwon Jang, Dongyoung Kim, and Jinwoo Shin. Dual-stream diffusion for world-model augmented vision-language-action model, 2025. URL <https://arxiv.org/abs/2510.27607>.
- [24] Chi-Lam Cheang, Guangzeng Chen, Ya Jing, Tao Kong, Hang Li, Yifeng Li, Yuxiao Liu, Hongtao Wu, Jiafeng Xu, Yichu Yang, Hanbo Zhang, and Minzhao Zhu. Gr-2: A generative video-language-action model with web-scale knowledge for robot manipulation. *arXiv preprint arXiv:2410.06158*, 2024.
- [25] Joel Jang, Seonghyeon Ye, Zongyu Lin, Jiannan Xiang, Johan Bjorck, Yu Fang, Fengyuan Hu, Spencer Huang, Kaushil Kundalia, Yen-Chen Lin, Loic Magne, Ajay Mandlekar, Avnish Narayan, You Liang Tan, Guanzhi Wang, Jing Wang, Qi Wang, Yinchen Xu, Xiaohui Zeng, Kaiyuan Zheng, Ruijie Zheng, Ming-Yu Liu, Luke Zettlemoyer, Dieter Fox, Jan Kautz, Scott Reed, Yuke Zhu, and Linxi Fan. Dreamgen: Unlocking generalization in robot learning through video world models, 2025. URL <https://arxiv.org/abs/2505.12705>.
- [26] Qingqing Zhao, Yao Lu, Moo Jin Kim, Zipeng Fu, Zhuoyang Zhang, Yecheng Wu, Zhaoshuo Li, Qianli Ma, Song Han, Chelsea Finn, Ankur Handa, Ming-Yu Liu, Donglai Xiang, Gordon Wetzstein, and Tsung-Yi Lin. Cot-vla: Visual chain-of-thought reasoning for vision-language-action models, 2025. URL <https://arxiv.org/abs/2503.22020>.
- [27] Jun Cen, Siteng Huang, Yuqian Yuan, Kehan Li, Hangjie Yuan, Chaohui Yu, Yuming Jiang, Jiayan Guo, Xin Li, Hao Luo, Fan Wang, Fan Wang, and Deli Zhao. Rynnvla-002: A unified vision-language-action and world model. *arXiv preprint arXiv:2511.17502*, 2025.
- [28] Jun Cen, Chaohui Yu, Hangjie Yuan, Yuming Jiang, Siteng Huang, Jiayan Guo, Xin Li, Yibing Song, Hao Luo, Fan Wang, Deli Zhao, and Hao Chen. Worldvla: Towards autoregressive action world model. *arXiv preprint arXiv:*, 2025.

- [29] Pengfei Zhou, Liliang Chen, Shengcong Chen, Di Chen, Wenzhi Zhao, Rongjun Jin, Guanghui Ren, and Jianlan Luo. Act2goal: From world model to general goal-conditioned policy, 2025. URL <https://arxiv.org/abs/2512.23541>.
- [30] Ruijie Zheng, Jing Wang, Scott Reed, Johan Bjorck, Yu Fang, Fengyuan Hu, Joel Jang, Kaushil Kundalia, Zongyu Lin, Loic Magne, Avnish Narayan, You Liang Tan, Guanzhi Wang, Qi Wang, Jiannan Xiang, Yinzhen Xu, Seonghyeon Ye, Jan Kautz, Furong Huang, Yuke Zhu, and Linxi Fan. Flare: Robot learning with implicit world modeling, 2025. URL <https://arxiv.org/abs/2505.15659>.
- [31] Wenyao Zhang, Hongsi Liu, Zekun Qi, Yunan Wang, Xinqiang Yu, Jiazhao Zhang, Runpei Dong, Jiawei He, He Wang, Zhizheng Zhang, Li Yi, Wenjun Zeng, and Xin Jin. Dreamvla: A vision-language-action model dreamed with comprehensive world knowledge. *CoRR*, abs/2507.04447, 2025. doi: 10.48550/ARXIV.2507.04447. URL <https://doi.org/10.48550/arXiv.2507.04447>.
- [32] Moo Jin Kim, Yihuai Gao, Tsung-Yi Lin, Yen-Chen Lin, Yunhao Ge, Grace Lam, Percy Liang, Shuran Song, Ming-Yu Liu, Chelsea Finn, and Jinwei Gu. Cosmos policy: Fine-tuning video models for visuomotor control and planning. *arXiv preprint arXiv:2601.16163*, 2026.
- [33] Yue Liao, Pengfei Zhou, Siyuan Huang, Donglin Yang, Shengcong Chen, Yuxin Jiang, Yue Hu, Jingbin Cai, Si Liu, Jianlan Luo, Liliang Chen, Shuicheng Yan, Maoqing Yao, and Guanghui Ren. Genie envisioner: A unified world foundation platform for robotic manipulation. *arXiv preprint arXiv:2508.05635*, 2025.
- [34] Yucheng Hu, Yanjiang Guo, Pengchao Wang, Xiaoyu Chen, Yen-Jen Wang, Jianke Zhang, Koushil Sreenath, Chaochao Lu, and Jianyu Chen. Video prediction policy: A generalist robot policy with predictive visual representations. *arXiv preprint arXiv:2412.14803*, 2024.
- [35] Shuang Li, Yihuai Gao, Dorsa Sadigh, and Shuran Song. Unified video action model. *arXiv preprint arXiv:2503.00200*, 2025.
- [36] Team Wan, Ang Wang, Baole Ai, Bin Wen, Chaojie Mao, Chen-Wei Xie, Di Chen, Feiwu Yu, Haiming Zhao, Jianxiao Yang, Jianyuan Zeng, Jiayu Wang, Jingfeng Zhang, Jingren Zhou, Jinkai Wang, Jixuan Chen, Kai Zhu, Kang Zhao, Keyu Yan, Lianghua Huang, Mengyang Feng, Ningyi Zhang, Pandeng Li, Pingyu Wu, Ruihang Chu, Ruili Feng, Shiwei Zhang, Siyang Sun, Tao Fang, Tianxing Wang, Tianyi Gui, Tingyu Weng, Tong Shen, Wei Lin, Wei Wang, Wei Wang, Wenmeng Zhou, Wenten Wang, Wenting Shen, Wenyuan Yu, Xianzhong Shi, Xiaoming Huang, Xin Xu, Yan Kou, Yangyu Lv, Yifei Li, Yijing Liu, Yiming Wang, Yingya Zhang, Yitong Huang, Yong Li, You Wu, Yu Liu, Yulin Pan, Yun Zheng, Yuntao Hong, Yupeng Shi, Yutong Feng, Zeyinzi Jiang, Zhen Han, Zhi-Fan Wu, and Ziyu Liu. Wan: Open and advanced large-scale video generative models. *arXiv preprint arXiv:2503.20314*, 2025.
- [37] Bo Liu, Yifeng Zhu, Chongkai Gao, Yihao Feng, Qiang Liu, Yuke Zhu, and Peter Stone. Libero: Benchmarking knowledge transfer for lifelong robot learning. *arXiv preprint arXiv:2306.03310*, 2023.
- [38] Tianxing Chen, Zanxin Chen, Baijun Chen, Zijian Cai, Yibin Liu, Zixuan Li, Qiwei Liang, Xianliang Lin, Yiheng Ge, Zhenyu Gu, et al. Robotwin 2.0: A scalable data generator and benchmark with strong domain randomization for robust bimanual robotic manipulation. *arXiv preprint arXiv:2506.18088*, 2025.

## A Appendix

### A.1 RoboTwin Detailed Results

Here we present the per-task results on RoboTwin evaluation in Table 3.

Table 3: Per-task success rates on RoboTwin under clean and randomized evaluation settings.

Task	Fast-WAM (Ours)		Fast-WAM-Joint		Fast-WAM-IDM		Fast-WAM w.o. co-train		LingBot-VA		$\pi_{0.5}$		Motus	
	Clean	Rand.	Clean	Rand.	Clean	Rand.	Clean	Rand.	Clean	Rand.	Clean	Rand.	Clean	Rand.
Adjust Bottle	100	100	98	99	94	99	98	100	90	94	100	99	89	93
Beat Block Hammer	99	97	100	98	98	98	80	92	96	98	96	93	95	88
Blocks Ranking RGB	100	100	100	100	100	99	88	86	99	98	92	85	99	97
Blocks Ranking Size	94	98	83	91	79	90	56	62	94	96	49	26	75	63
Click Alarmclock	100	100	100	100	98	100	100	98	99	100	98	89	100	100
Click Bell	100	100	100	98	100	96	100	100	100	100	99	66	100	100
Dump Bin Bigbin	97	96	95	95	93	98	92	94	89	96	92	97	95	91
Grab Roller	100	100	100	100	100	100	100	100	100	100	100	100	100	100
Handover Block	95	81	93	91	97	94	58	46	99	78	66	57	86	73
Handover Mic	99	100	100	100	98	99	100	100	94	96	98	97	78	63
Hanging Mug	58	62	71	56	66	62	28	40	40	28	18	17	38	38
Lift Pot	100	100	100	100	100	100	92	90	100	99	96	85	96	99
Move Can Pot	90	88	97	99	97	100	80	68	94	97	51	55	34	74
Move Pillbottle Pad	100	99	99	100	98	100	88	96	99	99	84	61	93	96
Move Playingcard Away	100	100	100	100	99	100	94	96	100	99	96	84	100	96
Move Stapler Pad	77	64	85	81	89	85	64	78	91	79	56	42	83	85
Open Laptop	98	100	89	92	92	92	100	98	92	94	90	96	95	91
Open Microwave	62	45	3	14	54	53	46	52	82	86	34	77	95	91
Pick Diverse Bottles	80	85	86	87	87	89	58	62	89	82	81	71	90	91
Pick Dual Bottles	100	96	98	99	100	98	80	74	100	99	93	63	96	90
Place A2B Left	95	93	96	96	97	96	84	92	97	93	87	82	88	79
Place A2B Right	93	99	95	95	94	98	88	84	97	95	87	84	91	87
Place Bread Basket	91	93	89	94	91	97	74	76	97	95	77	64	91	94
Place Bread Skillet	90	93	90	93	90	95	98	84	95	90	85	66	86	83
Place Burger Fries	96	99	100	100	97	99	94	96	97	95	94	87	98	98
Place Can Basket	71	69	50	23	37	28	72	72	81	84	62	62	81	76
Place Cans Plasticbox	99	96	98	98	98	96	98	96	100	99	94	84	98	94
Place Container Plate	96	100	99	98	100	96	94	98	99	97	99	95	98	99
Place Dual Shoes	94	88	93	89	85	87	80	74	94	89	75	75	93	87
Place Empty Cup	100	100	100	100	100	100	100	100	100	100	100	99	99	98
Place Fan	96	96	99	96	97	95	80	88	99	93	87	85	91	87
Place Mouse Pad	83	89	96	91	97	93	64	76	93	96	60	39	66	68
Place Object Basket	89	88	86	81	87	82	82	90	91	88	80	76	81	87
Place Object Scale	90	97	96	99	99	99	86	80	96	95	86	80	88	85
Place Object Stand	90	94	92	98	96	100	82	92	99	96	91	85	98	97
Place Phone Stand	97	99	100	100	99	99	90	92	97	97	81	81	87	86
Place Shoe	96	99	95	97	95	98	92	90	98	98	92	93	99	97
Press Stapler	90	97	52	50	50	57	80	80	85	82	87	83	93	98
Put Bottles Dustbin	95	90	93	95	97	92	78	88	87	91	84	79	81	79
Put Object Cabinet	94	89	95	90	93	90	88	84	85	87	80	79	88	71
Rotate QRcode	93	89	91	92	91	86	82	78	96	91	89	87	89	73
Scan Object	89	92	92	92	93	90	78	86	96	91	72	65	67	66
Shake Bottle	100	100	100	100	100	100	100	100	100	97	99	97	100	97
Shake Bottle Horizontally	100	100	100	100	100	100	100	100	100	99	99	99	100	98
Stack Blocks Three	95	97	98	97	99	95	90	90	99	98	91	76	91	95
Stack Blocks Two	100	100	100	100	100	100	100	98	100	98	97	100	100	98
Stack Bowls Three	80	81	84	86	85	83	66	82	86	83	77	71	79	87
Stack Bowls Two	92	98	97	95	94	96	90	98	94	98	95	96	98	98
Stamp Seal	90	94	96	99	99	94	60	78	96	97	79	55	93	92
Turn Switch	61	59	73	72	59	74	66	66	44	45	62	54	84	78
<b>Average</b>	91.88	<b>91.78</b>	90.84	90.32	91.16	91.34	82.76	84.80	<b>92.90</b>	91.50	82.74	76.76	88.66	87.02